Energy Buffer Dimensioning Through Energy-Erlangs in Spatio-Temporal-Correlated Energy-Harvesting-Enabled Wireless Sensor Networks

Raul Gomez Cid-Fuentes, *Student Member, IEEE*, Albert Cabellos-Aparicio, and Eduard Alarcón, *Member, IEEE*

***Abstract*—Energy-harvesting-enabled wireless sensor networks (EHE-WSN), despite their disruptive potential impact, still present several challenges precluding practical deployability. In particular, the low power density and random character of the ambient energy sources produce slow deep fadings in the energy that nodes harvest. Unfortunately, the capacity of the energy buffers is very limited, causing that, at some times, the node might interrupt its operation due to lack of stored energy. In this context, a general purpose framework for dimensioning the energy buffer is provided in this work. To achieve this, a dynamics-decoupled, multi-source capable energy model is presented, which can handle fast random patterns of the communications and the energy harvesting, while it can capture slow variations of the ambient energy in both time and space. By merging both dynamics, the model can more accurately evaluate the performance of the sensor node in terms of the energy storage capacity and to estimate the expected energy of the neighboring nodes. In order to evaluate the performance of the sensor node, a statistical unit for energy harvesting resources, referred as the Energy-Erlang (E2), has been defined. This unit provides a link between the energy model, the environmental harvested power and the energy buffer. The results motivate the study of the specific properties of the ambient energy sources before the design and deployment. By combining them in this general-purpose framework, electronics and network designers will have a powerful tool for optimizing resources in EHE-WSNs.**

***Index Terms*—Energy harvesting, energy management, negative-energy queue, system modeling, wireless sensor networks.**

I. Introduction

RECENT advancements in electronics [1]–[6] have pointed out that energy harvesting (EH), a process by which the energy derived from ambient or external sources [7] is captured and stored for later use in the sensor, is a firm candidate as a key enabling technology in the development of wireless sensor networks (WSNs) with perpetual character [8], [9]. The environmental energy can be harvested from a large variety of physical natures, such as solar [8], thermal, vibration [6], acoustic [10], or radio-frequency (RF) [2] energy sources.

These upcoming networks, referred as energy-harvesting-enabled wireless sensor networks (EHE-WSN), show unique properties not only because of their ultra low power constraints but also because of the fact that the energy state is time-varying. This is, the energy stored at the energy buffer is constantly increasing and decreasing in a random manner. In addition to this, the ambient energy has a slow temporal dynamic which modulates the harvesting power in several orders of magnitude. As an example, the available power of solar energy ranges from 10 $\mu\mathrm{W/cm^2}$ to up to 100 $\mathrm{mW/cm^2}$ a day [11]. Given the amount of factors which take part during the normal operation of any single node, it is challenging for the network designer to dimension critical parameters such as the link capacity [12], the energy buffer capacity of each sensor node, or to design transmission policies [13].

Among other critical parameters, the energy buffer, which is usually composed of supercapacitors or batteries, is one of the most expensive and larger volume subsystems. In particular, a typical supercapacitor requires an approximated volume of 2 $\mathrm{cm^3}$ in order to store 1 J of energy [14]. Thus, the design of the energy buffer might result either in an over dimensioning of its maximum capacity giving as a result significant downscaling impairments and an increase in cost, or, on the contrary, an under dimensioning, which would lead to unnecessary interruptions along the normal operation of the network.

In order to capture the random patterns of the energy harvesting process, existing energy models target one or another of the following challenges. On the one hand, the models presented in [12] and [15] model the energy source as an uncorrelated process in the communications time scale, thus the model can handle specific communication patterns. As a result, these models show that very low values of the energy buffer capacity (i.e., just a few tens of times the energy of a single data packet) is enough to maintain the communication. On the other hand, the models presented in [11], [16], [17] are aimed for solar energy harvesting and account for the daily temporal variations. In this case, these models cannot provide detailed information regarding the communication energy harvesting random patterns, but point out to energy buffer capacity to be of thousands to even millions times larger than the energy of a single data packet.

Manuscript received March 01, 2014; revised May 27, 2014; accepted June 26, 2014. Date of publication September 09, 2014; date of current version September 09, 2014. This paper was recommended by Guest Editor G. Wang.

The authors are with the N3Cat (NaNoNetworking Center in Catalunya), Universitat Politècnica de Catalunya (UPC), 08034 Barcelona, Catalunya, Spain (e-mail: rgomez@ac.upc.edu; acabello@ac.upc.edu; eduard.alarcon@upc.edu).

Color versions of one or more of the figures in this paper are available online at http://ieeexplore.ieee.org.

Digital Object Identifier 10.1109/JETCAS.2014.2337194

We consider that the large mismatch between models show a pending challenge which should be addressed.

In this context, we aim to provide an general purpose energy model, which can handle random patterns in both communications and energy harvesting processes, as well as it can provide realistic values when addressing slow temporal fadings in the available ambient energy. In addition, it must be of general purpose and multi-source capable, so that an arbitrary number of ambient energy sources can be evaluated. In order to do so, we present a novel dynamics-decoupled spatio-temporal energy model. This model is dynamics-decoupled since it models the energy harvesting as the product of two random processes with separated temporal dynamics: 1) the fast dynamics which is independent at each node and 2) the slow dynamics which models the spatial correlation among sensor nodes, as well as the fading times in the harvesting power, which cause that the nodes cannot temporarily achieve an energy-neutral operation [16]. Thanks to this model, it is possible to consider highly detailed information regarding the random patterns of the ambient energy sources and the communication process, while still taking in consideration the slow temporal variations.

In addition to that, we define the Energy-Erlang (E2) as a unit for energy utilization. The Energy-Erlang provides a link between the energy model, the environmental harvested power, the network requirements and the energy buffer capacity. Accordingly, we use the Energy-Erlangs to provide design guidelines in the design and dimensioning of the energy buffer capacity. In order to do so, we evaluate the performance of the sensor network in terms of the probability of energy outage. Finally, we evaluate the impact of the spatial correlation among sensor nodes in the correlation of the energy outage among neighboring nodes.

The rest of this paper is organized as follows. In Section II the energy path is described. In Section III the energy model is presented and the associated Energy-Erlang is defined. In Sections IV and IV-C, the energy model is evaluated in terms of the energy outage probability and the average time for an energy outage. In Section V we evaluate the spatial correlation of the energy outage. Finally, in Section VI we conclude our work.

II. Energy Path

In an energy-harvesting-enabled wireless sensor node, the energy which is used to enable the sensing, processing and communications is fully obtained from its close environment by means of ambient energy harvesters [7]. This energy would ideally present an ubiquitous and perpetual character, but it also generally has spatio-temporal-correlated properties [18]. Afterwards, this energy is conditioned in order to be stored in an energy buffer (e.g., a battery or a capacitor). Finally, this energy is used to power the sensing, processing and communications units [19]. This flow is here referred as the *energy path*.

The purpose of this section is two-fold. Firstly, we aim to provide an overview of the consisting sub-system parts of the energy path, and secondly, we present the basic assumptions and relations among parts, as well as we define the dynamics-decoupled model for the ambient energy.

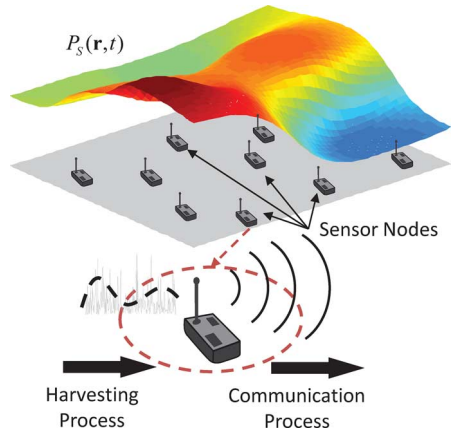

Fig. 1. Separation of dynamics. Energy field is correlated in both time and space. Harvesting energy is bursty and random but it presents a smooth variation in temporal average.

A. Ambient Energy

The ambient energy can be harvested from a very large variety of physical phenomena. In particular, the most appealing energy sources for energy harvesting range from solar, thermal, mechanical, acoustic, or RF. As it is shown in [7], the power that a sensor node can harvest depends upon many factors, such as nature of the source, power availability, and dimensions of the energy harvester.

Among other physical phenomena, solar, human movement, vibrations, or RF waves already present implementable transducers for sensors. In particular, the average power that it can be harvested from each energy source is in the order of 10 mW for solar, 1 mW for human movement, 10 μW for RF, and 1μW for vibrations [7]. However, the instantaneous power that it available at a given time and space is unpredictable.

In order to provide a model for the ambient energy, we require it to be as general as possible, we assume that the ambient energy, which is harvested, is spatio-temporal correlated and its value is given by what we define as the energy field. The energy field, $P_H(\mathbf{r},t)$ in power units, is defined as a spatio-temporal function which provides the energy that would be harvested in case that a node is located at a certain location $\mathbf{r}$ at a time t.

To avoid an overhead in notation, in what follows, we will refer as $P_H(\mathbf{r},t)$ the energy field, as $P_H(t)$ the power which is harvested from the energy field at the location of the sensor node under study and P_H as the average value of the energy field at the location of the sensor node.

Then, we assume that the energy field is given by the product of two separated dynamics

$$P_H(\mathbf{r},t) = P_S(\mathbf{r},t) \cdot p(\mathbf{r},t) \tag{1}$$

where $p(\mathbf{r},t)$ is a dimension-less, spatio-temporal-decorrelated random process, referred as the fast dynamics, and $P_S(\mathbf{r},t)$, in power units, stands for a random process with a slow variation in time as well as in space, here referred as the slow dynamics. The coexistence of these two dynamics is shown in Fig. 1.

The large temporal difference between both dynamics is such that it is accomplished that the average in time of P_H, can be separated by the product of both time-averages

$$\langle P_H(\mathbf{r})\rangle = \langle P_S(\mathbf{r})p(\mathbf{r})\rangle = \langle P_S(\mathbf{r})\rangle \cdot \langle p(\mathbf{r})\rangle \tag{2}$$

where the $\langle\cdot\rangle$ operator stands for time average. Provided that the above equation holds, it is then obtained that we can approximate $P_H(\mathbf{r},t)$ at a time close to t_0 as

$$P_H(\mathbf{r},t) \approx P_S(\mathbf{r},t_0)p(\mathbf{r},t) \tag{3}$$

for short time intervals, such that $P_S(\mathbf{r},t_0)$ can be considered constant within a node, while we can approximate P_H as

$$P_H(\mathbf{r},t) \approx P_S(\mathbf{r},t) \tag{4}$$

for long time intervals. Therefore, depending on the length of the time interval, we can approximate the energy harvesting by just considering either the fast or the slow dynamics.

In addition, we define as e_H (and E_H its averaged value) the harvested energy over a fixed time T_H

$$e_H = \int_{T_H} P_H(t)dt \tag{5}$$

and alternatively, we define t_H (and thus, T_H its averaged value) as the time such that a given fixed amount of energy E_H has been harvested

$$t_H \equiv \text{time s.t.} \int_{t_H} P_H(t)dt = E_H. \tag{6}$$

The spatio-temporal correlation of the slow dynamics is modeled with a correlation coefficient. As a general definition, the correlation coefficient of the harvested power between the nodes i and j, located at $\mathbf{r_i}$ and $\mathbf{r_j}$ at times t_i and t_j respectively is given by

$$\rho_{ij}(\mathbf{r_i},\mathbf{r_j},t_i,t_j) = \\ = \frac{E\left[(P_H(\mathbf{r_i},t_i) - \langle P_H(\mathbf{r_i})\rangle)(P_H(\mathbf{r_j},t_j) - \langle P_H(\mathbf{r_j})\rangle)\right]}{\sigma_H(\mathbf{r_i})\sigma_H(\mathbf{r_j})} \tag{7}$$

where $\sigma_H(\mathbf{r_i})$ and $\sigma_H(\mathbf{r_j})$ refer to the standard deviation of the energy field at the locations of the nodes i and j.

Finally, we define the coherence time, t_c, as the minimum average time at which two points present no correlation between them. The concept of coherence time will result very helpful in the following sections in order to relate how fast the energy field varies in time and the impact that it has over the evaluated results.

B. Energy Buffer

By following the energy path, the harvested energy is temporarily stored in an energy buffer, until this is used by the communication unit of the sensor node. This sub-unit is generally composed of a battery or supercapacitors and it is one of the most expensive and volume consuming of the sub-units contained within a node. In particular, typical batteries present an energy density in the order of 0.2 MJ/kg and recharging cycles in the order of 1000. Alternatively, supercapacitors show larger and faster recharging cycles, at the expense of a more reduced energy [7], [14].

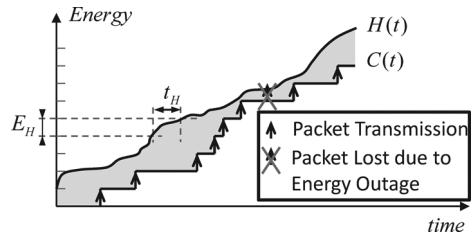

Fig. 2. Depiction of the three elements which interact in the energy path. Harvested energy, the energy stored in the energy buffer and the energy used for communications.

An additional challenge in energy storage technologies, which also motivates the minimization of the energy buffer, is the energy buffer leakage [19]. This impairment depends of the energy buffer capacity, which typically results in over-dimensioned energy buffers, limiting the optimal operation of the sensor node. However at the same time, large energy buffers suffer from larger losses and in some cases, the leakage consumes more energy than the communication subsystem.

This energy buffer of maximum capacity C_B, in energy units, (e.g., a battery or a supercapacitor) will store energy while absorbing the time-varying random variations of both the energy harvesting and communication processes. We define the energy state, $s(t)$, as the energy which is stored at a time t in the energy buffer. This is a random process, which, in turn, is a function of the energy harvesting and the communication processes. This is given by

$$\frac{\partial}{\partial t}s(t) = P_H(t) - P_C(t) - P_L(t) \\ \text{Subject to}: 0 \le s(t) \le C_B \ \ \forall t \tag{8}$$

where $P_H(t)$ is the power which is harvested at the node location, $P_C(t)$ stands for the power which is requested by the communications unit and $P_L(t)$ refers to the power losses.

For a better understanding of the three elements which interact in the energy path, they are shown in Fig. 2. $H(t)$ refers to the aggregation of the energy which is harvested starting from the time $t = 0$ plus the initial stored energy. $C(t)$ stands for the aggregated energy which has been used for communications. In addition, the energy which is stored in the energy buffer, $s(t)$, is represented as the shaded area between the curves $H(t)$ and $C(t)$. Finally, we have also represented the data transmission requests as arrows.

C. The Communications Unit

The communication process in a WSN is characterized by the transmission of short data packets. A data packet has an associated energy, e_C (E_C in average), which is required in order to guarantee that the transmitted data can be recovered at the receiver node. This energy, e_C, is a function of the link capacity, the distance between nodes and the transceiver constraints, as provided by Shannon's link capacity.

The packetized patterns of the communications unit enables the discretization of (8). Such discretization has been performed in previous works [11], [12] by providing a Markov chain.

III. Negative-Energy Queue Model

A. State-of-the-Art Models

The existing state-of-the-art joint models, which are based on Markov queues, can be roughly classified into three types. In the first type the basic unit is the energy packet and, unlike classical communications queues, empty queues of energy packets entail an interruption of the normal operation of the sensor nodes. In such models the energy harvesters generate arrivals of energy packets that in turn, are stored in the energy buffer (representing a battery or a supercapacitor). The communication unit is modeled as a server which processes the energy packets where the service time is associated to the generation of communications events[15], [20], [21]. The second type of models proposes the interconnection of two different Markov chains, namely a main queue for communications packets and a secondary queue for energy harvesting resources. Such type of models consider that a data packet can be effectively transmitted when it has been processed by the main queue and the queue of energy-packets is not empty [12], [13]. And finally, the third type are based on state-dependent Markov chains where each state represents a combination of the amount of energy, data packets available in their respective buffers [22]–[24].

Alternatively, existing joint models for solar energy harvesting account for daily temporal variations of the ambient energy. Due to the fact that solar energy provides a significantly larger amount of energy, and due to the fact that sensor nodes must store enough energy for several hours, these models are very source-specific, and therefore not general purpose [11], [16], [17].

Overall, existing joint energy/information models suffer from a remarkable degree of complexity, at the same time extending them to account for multi-source energy harvesting systems is challenging since the energy harvesters are not considered as individual entities. Furthermore, they are not typically equivalent to classical communication models and as such, harder to solve. The goal of this paper is to develop a new type of model that it is simple, accurate and that naturally accounts for the multi-energy harvesting environment.

B. Negative-Energy Queue Model

Given the large amount of literature devoted to queue theory for communication models, we consider that a queue model for EHE-WSN nodes should have the same properties than a communication queue. That is, we pursue an energy model such that:

- the stability condition must be $\rho < 1$;
- the idle state must be defined as the state of having an empty queue;
- the loss of communication must be assigned to a full queue.

Thanks to such queue model, we would be capable of using the well known results and closed-form expressions for communications, and to translate them into energy harvesting requirements.

Therefore, we define the negative-energy queue model for EHE-WSN as in Fig. 3. As it is shown, the arrivals of this queue are generated by the set of applications of the sensor node. i.e., every time an application spends one unit of energy, it generates

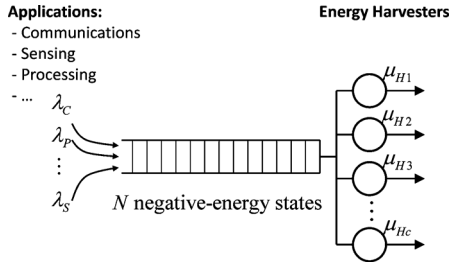

Fig. 3. Negative-energy queue model. Model consists of arrivals of negative-energy packets which are produced as the applications consume energy from the energy buffer. Negative-energy packets are processed by the energy harvesters. Negative-energy queue model provides a very simple framework to model a sensor node with multiple power consuming applications and multiple energy harvesters.

an arrival of negative-energy. Each type of application has an associated generation rate (e.g., λ_C for communications, λ_P for processing and λ_S for sensing). On the other hand, the service time, $T_H = 1/\mu_H$, is the time that an energy harvesting unit needs to process one negative-energy packet. In other words, T_H is the time that it takes for the energy harvesting unit to harvest the required amount of energy that has been consumed by a certain application (6).

In order to account for power losses [19] in our negative-energy queue model we assume them as constant. This assumption is valid for a wide set of values of the energy buffer state while does not apply for very low or very high energy buffer states [25]. Below a certain threshold of stored energy the sensor node stops its operation, this is taken into account by our model as a full negative-energy queue. Similarly, the energy harvested by sensor nodes with very high energy stored is lost because of the leakage, this represents the maximum achievable capacity of the energy buffer. We consider this case in our model as an empty negative-energy queue.

In addition to this, recent trends in sensor node design is pointing to multi-source energy harvesting [6], [26], [27]. Multi-source energy harvesters can be considered in this queue model by connecting them in parallel, such as multiple servers in a communication queue (e.g., M/M/c/N and M/G/c/N).

Finally, the queue of negative-energy packets refers to the energy buffer but observed upside down. A queue which is empty of negative-energy packets refers to a fulfilled energy buffer, while a fulfilled queue stands for an empty energy buffer. Thus, the number N of negative-energy states is related to the energy buffer capacity as

$$N = \frac{C_B}{E_H} \tag{9}$$

where C_B is the energy buffer capacity and E_H refers to the energy which is harvested over a time T_H. Additionally, if at a certain time t_k the queue has L^k negative-energy packets, then the energy state s^k at the energy buffer is given by

$$s^k = C_B - L^k E_H. \tag{10}$$

It is observed that when the queue does not have any negative energy packet, the energy harvester unit can remain in idle state, alike communications queues.

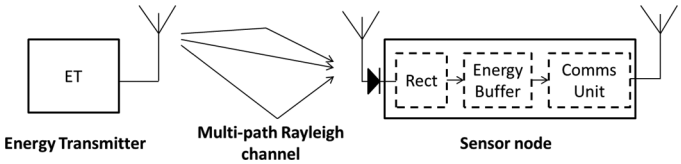

Fig. 4. Set-up of the time-domain simulation.

For further evaluation along this work, we have considered communications processes, with Poisson arrivals, as the generator of negative-energy packets and a single energy harvester. Therefore, as it follows, we can use the literature of M/G/c/N queues, so that we can evaluate the system for any arbitrarily chosen statistic distribution for the energy harvesting source.

C. The Energy-Erlang

By having provided the negative-energy queue model for EHE-WSN, we can now define the energy utilization as

$$\rho_E = \frac{\sum\limits_i \lambda_i}{\mu_H} = \frac{\sum\limits_i P_i}{P_H} \tag{11}$$

in Energy-Erlang [E2] units. As it can be observed, the energy utilization of the negative-energy queue model, unlike the utilization which was defined in typical queue models for EHE-WSN, is now stable for $\rho_E < c$, where c stands for the number of energy harvesters.

In general terms, the Energy-Erlang is a dimension-less unit which is proposed here as a statistical unit of energy harvesting resources.

As an example, let us assume that an energy harvester is able to harvest $P_H = 10\ \mu$W. If, in order to communicate, it requires $P_C = 25\ \mu$W, then the required energy harvesting resources result in $\rho_E = 2.5$ Energy-Erlangs, which means that at least three energy harvesters are required in order to enable a correct operation of the sensor node $(\rho_E < c)$.

Due to the fact that the Energy-Erlang is a ratio between the available and the required energy resources, it provides significant advantages in the design and dimensioning of sensors. In particular, this can be used to dimension energy harvesters, since we can relate the required harvesting power to meet certain user-defined requirements by $P_H = P_C/\rho_e$. In addition to this, it is also possible to dimension energy buffers for fixed available energy and requirements, through the evaluation of the negative-energy queue model. This is provided in the following sections through the evaluation of the energy outage probability.

D. The Energy Outage

As a metric for evaluation of the energy model to provide guidelines in dimensioning of energy buffer, we define the energy outage. The energy outage is defined as the time interval during which the sensor node does not have enough stored energy, and thus its operation is temporarily interrupted. This situation can be observed in Fig. 2. The probability that this occurs equals to the probability that the queue of negative-energy is full, and so, it equals to the expression for blocking probability of a queue model for communications [28]. Therefore, by means of queue theory on M/G/1/N, we can obtain that the outage probability, p_{out} is given by

$$p_{\text{out}} = P_N = 1 - \frac{1}{\pi_0 + \rho_E} \tag{12}$$

where π_0 refers to the probability that there are 0 negative-energy packets left within the queue right after the last negative-energy packet was processed by the energy harvester. π_0 is found as a solution for

$$\pi_n = \sum_{n=0}^{N-1} \pi_j p_{jn}, \quad 0 \le n \le N-1$$

and

$$\sum_{n=0}^{N-1} \pi_n = 1 \tag{13}$$

where, equivalent to π_0, π_n refers to the probability that there are n negative-energy packets left and p_{jn} stands for the state transition probability of remaining negative-energy packets from the state j to the state n, considering each state right after a negative-energy packet has been processed by the energy harvester.

IV. Evaluation of the Energy Outage

In this section we evaluate the energy outage probability in terms of the utilization in Energy-Erlangs and the normalized energy buffer capacity. This evaluation considers two representative cases, which are single-source energy harvesting systems and the recently proposed multi-source energy harvesting platforms [6], [26], [27].

A. Evaluation of the Fast Dynamics

1) Time-Domain Simulation Set-Up: In order to validate the negative-energy queue model, we have first performed a time-domain simulation which implements a one-to-one transmission of RF energy in a multi-path environment. The energy transmitter (ET) generates an RF wave, which is propagated through a multi-path Rayleigh channel with coherence time $t_c = 0.5$ s [29], the average power at the receiving node is set to 10 μW, which is reasonable as reported in [30]. A block diagram of the simulation set-up is shown in Fig. 4. At the receiving node, a rectenna is used to harvest the energy of the RF wave [2]. The power which is harvested is power processed and stored in a continuous manner in an energy buffer of variable capacity. The communications unit transmits data packets with a variable Poisson distributed inter-arrival rate.

2) Negative-Energy Model Simulation Set-Up: In order to model the fast dynamics, we assume that the energy harvester processes these negative-energy packets at a rate of $\mu_H = 1$ negative-energy packets per second, following both Poisson and chi-squared statistics. Then, the communications unit generates Poisson arrivals of negative-energy packets at a rate of $\lambda_C = \rho_e/\mu_H$.

A Poisson distribution might not hold as a general case, however it studied due to two main reasons. Firstly, the energy

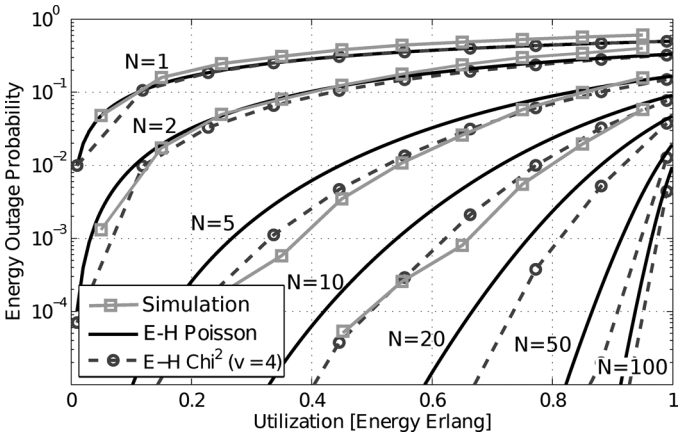

Fig. 5. Comparison between the energy outage probability obtained by assuming a Poisson process for the energy harvesting and by assuming that the energy harvesting process is chi-squared distributed. It is shown as a function of the energy utilization for different values of the normalized energy buffer capacity.

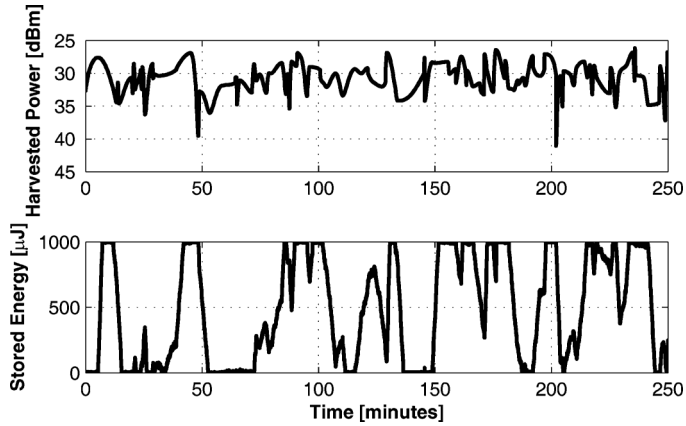

Fig. 6. Model of the Rayleigh channel and evolution of the energy state at the sensor node.

outage probability has a closed-form expression, which is given by

$$p_{\text{out}} = \frac{1-\rho_E}{1-\rho_E^{N+1}}\rho_E^N. \tag{14}$$

And, secondly, a Poisson process has very large entropy [31], thus becoming the energy outage probability of a M/M/1/N as an upper bound in the energy outage probability in many environments.

Alternatively, a chi-squared distribution is of special interest in the context of energy harvesting, since this distribution is given as a result of harvesting energy from a Gaussian noise-like energy source [32]. In particular, the energy which is harvested during a time T from a Gaussian noise-like source of bandwidth W is modeled as chi-squared distribution with $k = 2TW$ degrees of freedom. In this simulation, we have chosen $k = 4$, since it is the result of approximating the time-domain simulation parameters with a time $T = 1/\mu_H$ and $W = 1/t_c$.

3) Performance Evaluation and Comparison: In Fig. 5 we compare, in terms of the energy outage probability, the time-domain simulation results to the negative-energy queue model results assuming 1) a Poisson distribution for the energy harvesting process (black continuous lines) and 2) a chi-squared distribution for the energy harvesting process. The energy outage is evaluated as a function of the energy utilization for different values of the normalized energy buffer.

As the results show, the negative-energy model well predicts the behavior of time-domain simulation, although significantly reducing the computational cost. In addition, we observe that the energy outage probability is upper bounded by the results from the M/M/1/N queue and it tends to $p_{\text{out}} = 1/(N+1)$ when the energy utilization tends to one. As an example, if considering that the sensor node has the following requirements: $E_C = 10\ \mu$J, $\lambda_C = 0.9$ packet/s, and the node is able to harvest $P_H = 10\ \mu$W from an environmental source, then we find that the energy utilization equals to $\rho_E = 0.9$ E2. By considering a target of $p_{\text{out}} = 10^{-2}$ in the energy outage probability, it is obtained that we would require a normalized energy buffer capacity of $N = 20$. Finally, if we express the energy buffer capacity in terms of energy, we would require an energy buffer capacity of $C_B = 200\ \mu$J.

B. Evaluation of Joint Dynamics

In a real environment, the ambient energy is time-varying. This is, the actual harvesting rate slowly evolves with time in an unpredictable manner, within a wide range of orders of magnitude. As a result, the power which is being harvested at the node location is affected by deep fadings.

Given the large variety of ambient energy sources, in this section we focus on RF energy harvesting affected by multi-path propagation. It is well known that multipath propagation is a very common effect during the reception of RF power within an urban area. The multipath is defined as the propagation of an RF signal through two or more paths, giving as a result constructive or destructive interference and phase shifting. When the number of interferences is large and it is very environment-dependent, the received power is affected by the Rayleigh fading [29]. In general terms, this model is mainly characterized by a certain coherence time, t_c, or, equivalently, with the doppler frequency.

In Fig. 6 we show an example of the harvested power, $P_H(t)$ over time when assuming that the harvesting source is affected by the Rayleigh channel. In addition, it is also shown a depiction of the energy state at the energy buffer of the sensor node. As it is shown, given the variation of the harvested power, the energy state is unable to reach a steady-state. On the contrary, deep fadings tend to completely deplete the energy buffer. Alternatively, when the multipath propagation provides constructive interference, the sensor node is able to store large amounts of energy.

Thus, in consideration of the multipath propagation, it is observed that the energy buffer does not only have to store enough energy to handle the random patterns of both communication and energy harvesting processes, but it also does have to be able to store large enough amounts of energy to overcome deep fadings in the harvested energy.

The lack of a steady state leads to evaluate the energy outage probability throughout event-based simulation of the negative-energy queue. In order to do so, we have assumed that the average energy harvesting rate, μ_H, evolves in time by following a Rayleigh distribution. The temporal evolution of μ_H is related

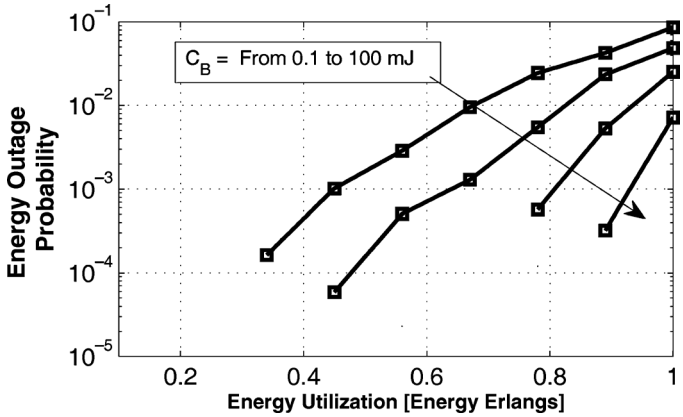

Fig. 7. Energy outage probability assuming Rayleigh fading with coherence time $t_c = 10$ s as the slow dynamics in the energy harvesting power source. An average $P_H = 10\ \mu$W and $E_C = 10\ \mu$J has been assumed in order to obtain these results.

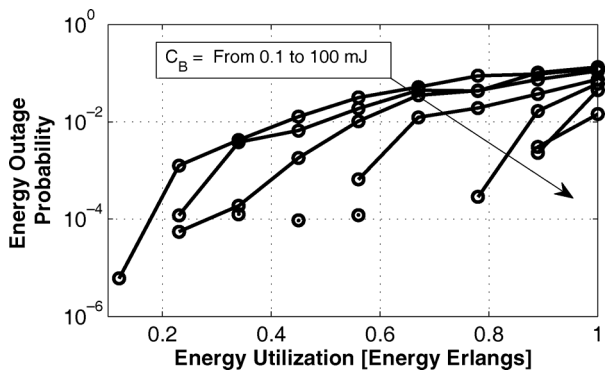

Fig. 8. Energy outage probability assuming Rayleigh fading with coherence time $t_c = 100$ s as the slow dynamics in the energy harvesting power source. An average $P_H = 10\ \mu$W and $E_C = 10\ \mu$J has been assumed in order to obtain these results.

to the coherence time, t_c. In Figs. 7 and 8, we show the results of the energy outage probability as a function of the energy utilization in Energy-Erlangs, for different values of the energy buffer capacity. In order to obtain these results, the average ambient power has been set to $P_H = 10\ \mu$W and the energy per packet has been set to $E_C = 10\ \mu$J. As it is shown, the effect of the slow dynamics is clear. While in Fig. 5, an energy buffer of 200 μJ was enough to guarantee a $p_{\text{out}} < 10^{-2}$ for $\rho_E = 0.9$ E2, in this case, by assuming slow dynamics, we would now require an energy buffer of 5 or 50 mJ to meet the same requirements for $t_c = 10$ s and $t_c = 100$ s, respectively.

As we would expect, the most critical situation refers to an energy utilization of $\rho_E = 1$ E2. That is, the communications unit requires the whole amount of energy which is harvested. As it is shown in the previous figures for both dynamics, this case has for any energy buffer capacity the worst energy outage probability. In Fig. 9, we show the energy outage probability of the sensor node in terms of the energy buffer capacity. As it can be observed, by increasing the size of the buffer, the node is able to temporarily store more energy to satisfy the energy requirements for larger fadings. It is found that the relation between the buffer size and the energy outage probability follows an exponential relationship.

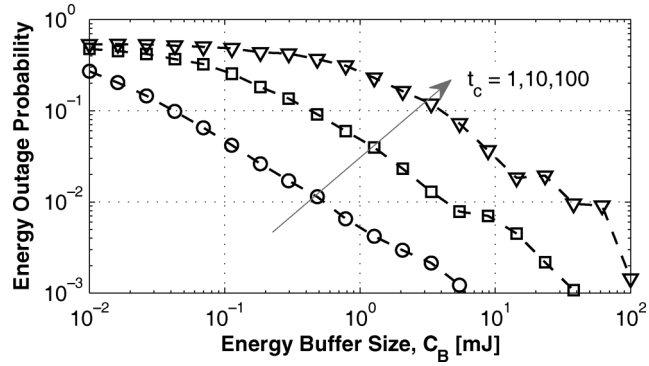

Fig. 9. Dependency of the energy outage probability in terms of the energy buffer size. It is represented for three different coherence times of the energy source: 1, 10, and 100 s.

C. Average Time to Energy Outage

Another relevant parameter which is set as a metric for design and dimensioning of energy buffers is the average time to energy outage. This metric evaluates the average time it takes for the node to fail in the communication due to energy outage. This time has large implications in the network protocol designs, such as routing. As an example, when a node is temporarily disconnected from the network, any existing route which would go through this node must be reassigned to neighboring nodes. Then, a larger average time to the energy outage represents a reduction in the network reconfiguration, and thus it represents a reduction in communication, control and energy overhead. In fact, a similar concept in battery-powered WSNs is defined. The network lifetime in a WSN is defined as the time it takes for any node to deplete its battery, thus causing an alteration in the network topology.

In Figs. 10 and 11 we show the average time to energy outage as a function of the energy utilization in Energy-Erlangs, for different values of the energy buffer capacity, considering a coherence time of $t_c = 10$ s in Fig. 10 and a coherence time of $t_c = 100$ s in Fig. 11. In order to obtain these results, we have set the same parameters as in the evaluation of the probability of energy outage. As it is shown, the average time to energy outage rapidly decreases as the energy utilization tends to one. On the contrary, this time increases rapidly for larger energy buffer capacity, thereby establishing a relevant design guideline.

In addition to this, for a better understanding on the dependence of the energy buffer capacity on the average time to energy outage, we show in Fig. 12 this average time as a function of the energy buffer for a coherence time of $t_c = \{10, 100, 1000\}$ s. As it is shown, channels with large temporal correlation need larger energy buffers in order to overcome long deep fadings. Interestingly, it is observed that for small sizes of the energy buffer, the average time to energy outage tends to the coherence time. However, as the energy buffer capacity is increased, the average time increases faster for those environments with smaller t_c.

D. Multi-Source Energy Harvesting

As mentioned in the previous section, this model is also capable of handling multi-source energy harvesting platforms. These platforms are gaining interest as they provide a robust

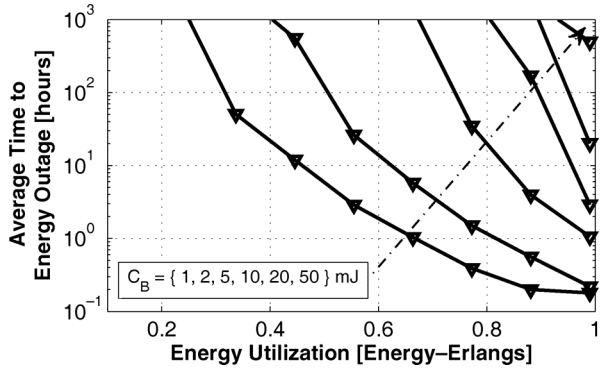

Fig. 10. Average time to energy outage assuming Rayleigh fading with coherence time $t_c = 10$ s.

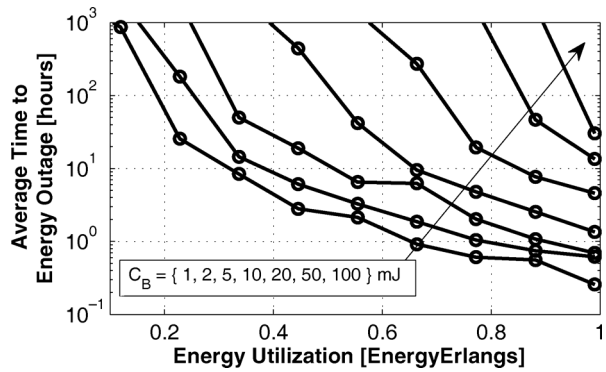

Fig. 11. Average time to energy outage assuming Rayleigh fading with coherence time $t_c = 100$ s.

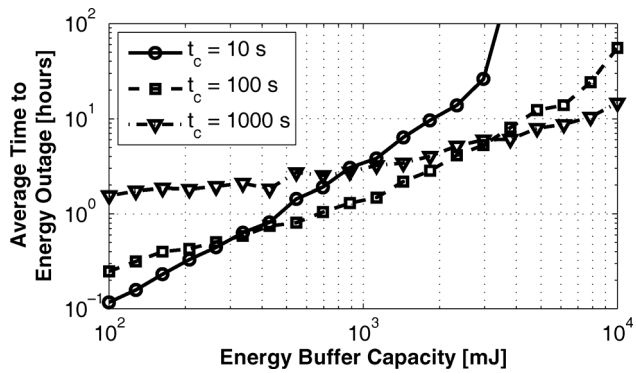

Fig. 12. Average time to energy outage assuming Rayleigh fading with coherence as a function of the energy buffer capacity.

alternative to power wireless sensors, since the sensor node can maintain its operation regardless of the fact that one of its energy sources might be temporarily unavailable [6], [26], [27], into better cope with time asynchronicity [33].

For this, the major benefits of these platforms are found in environments where the available power is presented with a sparse slow dynamics, since the combination of independent energy sources reduces the overall sparsity, thus potentially minimizing the chances of being affected by a deep fading.

Due to the fact that multi-source energy harvesting are of interest in energetically sparse environments, we have approximated a sparse ambient energy by a random process generated by exponentially distributed energy bursts of power $P_H C/c$,

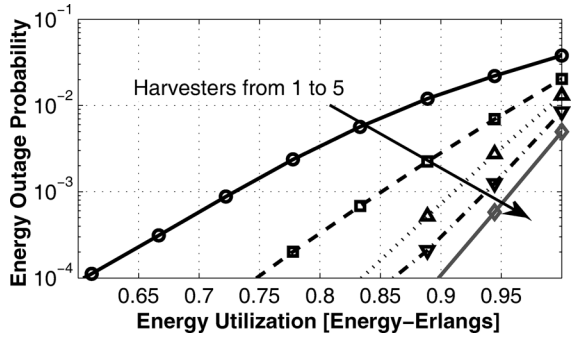

Fig. 13. Energy outage probability as a function of the energy utilization. $C_B = 10\text{mJ}$ and $C = 10$.

where C refers to the power crest factor and c stands for the number of harvesters. The inter-burst time has been set to $100/C$ s, modeled with an exponentially distributed random process. Therefore, the length of the burst is set such that, in average, each harvester is able to receive $P_{Hi} = P_H/c$. The power crest factor, C, is defined as

$$C = \frac{\overline{P_{\text{peak}}}}{P_H} \tag{15}$$

where $\overline{P_{\text{peak}}}$ is the average peak power.

Fig. 13 compares the energy outage probability in terms of the number of harvesters, as a function of the normalized energy utilization, defined as ρ_e/c, also in Energy-Erlang units. In order to obtain these results, the energy buffer capacity has been set to $C_B = 10$ mJ and the power crest factor has been fixed as $C = 10$. As the comparison shows, considering multi-source energy harvesters has a very positive impact upon the performance of the sensor node, when considering large power crest factors. In particular, it is possible to reduce down to two orders of magnitude the energy outage probability, while maintaining the same user-defined requirements in terms of the energy utilization.

E. Dimensioning Guidelines

In order to provide guidelines to enable an uninterrupted operation of the sensor nodes, we observe that there exist a trade-off in the design of the energy buffer, the energy harvesting unit and the communications capabilities, since operating with low values of energy utilization (i.e., the harvesting power is larger than the actually used) reduces the energy buffer capacity.

Due to the fact that the energy utilization is a ratio, the Energy-Erlang can be used to define the energy harvesting requirements for fixed communications capabilities ($P_H = P_C/\rho_e$). In this case, the trade-off between energy buffer and energy harvesting sub-units can be studied to minimize their overall area/cost [33]. As an example, in Fig. 7 it is observed that in order to provide a $p_o ut = 10^{-3}$, an energy buffer of 100 mJ is required for an energy utilization of $\rho_e \approx 0.9$, whereas only an energy buffer of 0.1 mJ is required in case that the energy utilization is reduced down to $\rho_e \approx 0.45$. In other words, for a fixed communications capabilities, the energy buffer capacity has been reduced in three orders of magnitude at the cost of doubling the energy harvesting requirements.

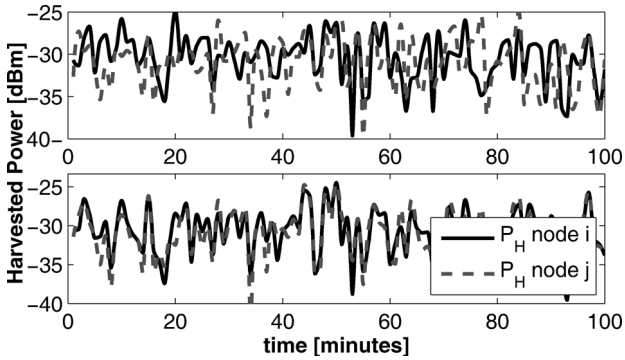

Fig. 14. Correlation of the ambient energy: comparison of the harvested power in two neighboring nodes with spatial correlation $\rho_d = 0.155$ (top) and $\rho_d = 0.844$ (bottom).

V. Spatial Correlation of the Energy State

In previous sections, the energy outage has been addressed for just a single sensor node. It has been assumed that the sensor node can transmit any time it has enough energy to transmit. Intuitively, in order to successfully deliver a data packet from the node i to the node j, not only the transmitter node must be energetically charged, but also the receiver must be active.

In this section, we evaluate the correlation of the energy outage probability of neighboring nodes. In order to do so, this work accounts for the spatial correlation of the energy field. The spatial correlation, ρ_d, defined as a function of the distance between nodes can be simplified from (7), if considering only spatial variations by

$$\rho_d(d) = \frac{E\left[P_H(\mathbf{r_i})P_H(\mathbf{r_j})\right] - \mu_H^2}{\sigma_H^2} \tag{16}$$

where $d = \|r_i - r_j\|$ refers to the distance between nodes i and j, and μ_H refers to the average power of the ambient energy source. The spatial correlation as a function of the distance is assumed to decrease monotonically with the distance and bounded to 1 when $d = 0$ and 0 when $d \to \infty$. This spatial correlation depends upon the physical phenomena, which can be generally classified into several groups [34], [35], e.g., spherical, power exponential, rational quadratic, or *matérn*. As an example of physical phenomena, electromagnetic waves present a power exponential correlation function, with $\theta_2 = 1$ [36]. The exponential correlation function is given by

$$\rho_d(d) = e^{(-d/\theta_1)^{\theta_2}}; \quad \theta_1 > 0, \theta_2 \in (0, 2]. \tag{17}$$

In order to evaluate the correlation of the energy outage among neighboring nodes, we focus on a RF energy harvesting environment, where the correlation of the slow-dynamics of the harvesting energy between two locations is given by (17). Then, we use a Rayleigh channel model from Section IV. To evaluate this correlation, we proceed to simultaneously perform a time-varying simulation of two neighboring nodes which harvest correlated RF power. Fig. 14 shows an example of the harvested power from two neighboring nodes when there is a spatial correlation of $\rho_d = 0.15$ (top) and $\rho_d = 0.85$ (bottom).

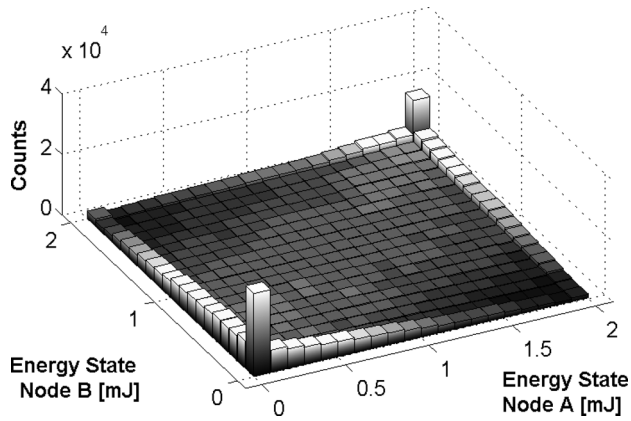

Fig. 15. Energy state correlation between two nodes, for a correlation factor of $\rho_d = 0.4$.

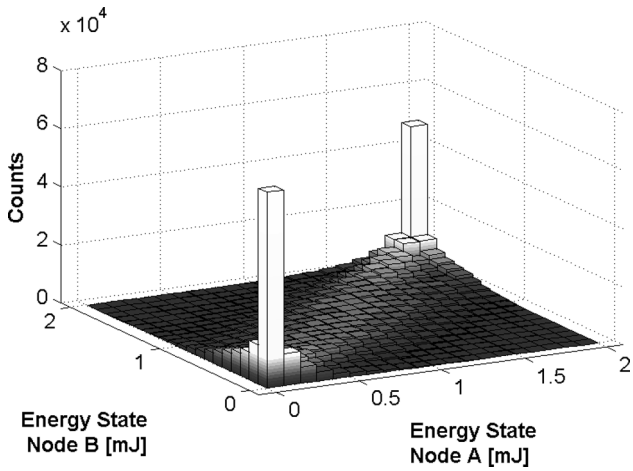

Fig. 16. Energy state correlation between two nodes, for a correlation factor of $\rho_d = 0.9$.

In Figs. 15 and 16, we show the bivariate histogram of the energy state of two energy harvesting enabled sensor nodes which present a correlation in their harvesting rates of $\rho_d = 0.4$ and $\rho_d = 0.9$. In order to obtain these results, an energy buffer capacity of $C_B = 2\,\mathrm{mJ}$ has been chosen. As shown, the relatively small capacity of the energy buffer, leads to a noticeably large probability of energy outage. As it is also observed, as the correlation of the energy source decreases, the bivariate histogram the energy states spreads, thus becoming challenging to estimate the energy state of neighboring sensors.

In addition to this, Fig. 17 shows the probability that a certain node j is in energy outage, when it is known that the node i is already in energy outage. This probability is shown as a function of the distance, when considering the values of $\Theta_1 = 5$ and $\Theta_2 = 1$ in the correlation model shown in (17). As the figure shows, at short distances, if a node is in energy outage, neighboring nodes of this sensor node will probably be in energy outage as well. Alternatively, as the distance among nodes increases, this probability tends to the energy outage probability. Alike temporal variations of the slow dynamics, the energy buffer has a significant effect in counteracting the impact of the spatial distribution of the energy.

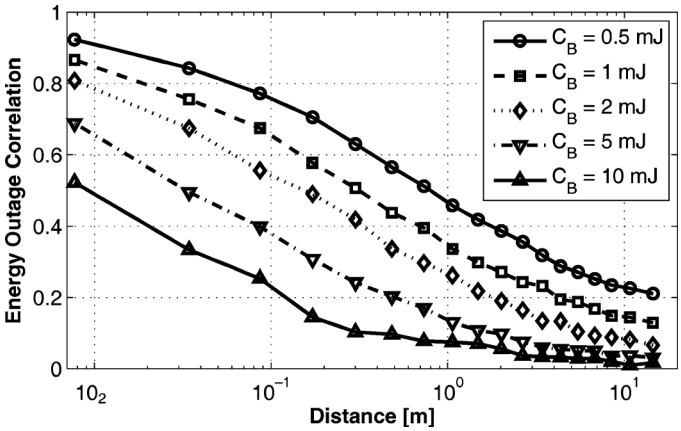

Fig. 17. Correlation of the energy outage probability in terms of the correlation among sensor nodes.

A. Applications of the Spatial Correlation

The correlation of the environmental energy and the energy state of the sensor nodes is of special interest for network designers. As an example, in the MAC-layer, sensors can increase the success rates in packet delivery in a point-to-point communication, since they can estimate whether the destination node has sufficient energy to receive the packet.

However, we expect that the majority of the benefits of this model will lay on the routing layer. State-of-the-art routing protocols for energy harvesting include the energy state in their cost function [37]–[39]. With this, the network tries to avoid nodes which have significantly less remaining energy and, therefore extending the network operation. When considering spatially distributed energy fields, routes bend to energetic networking areas [38]. This aims to balance the overall energy availability to the energy requirements.

Unfortunately, in order to optimize the routes in these environments, the network must take decisions upon the up-to-date energy state and energy availability of the sensors. As a result, this information must be constantly exchanged among nodes—or, even, reported to the base station (BS)—to generate the optimal solutions.

In this context, having knowledge of the spatial distribution of the ambient energy and the correlation among energy states can improve the network operation: on the one hand, sensor nodes can potentially take decisions on behalf of their neighboring nodes, thus suppressing the local exchange of overhead information. On the other hand, in case of reporting the energy state to a BS, the reporting overhead can be also reduced, since fewer nodes are required to report updated information.

VI. Conclusion

Energy harvesting will have a great impact in the deployment of WSNs. However, there are still many unsolved challenges. Regarding the design of the energy buffer, it has been shown that there is a strong compromise between size and achieving an uninterrupted operation. Up to now, the dimensioning of the energy buffer has still been a pending challenge, which has been usually solved by over-dimensioning. In this paper, a novel spatio-temporal energy model has been presented, which considers the separation of dynamics. Through this energy model, the random patterns of the ambient sources, the communications, and the energy state, as well as the impact of slow fadings in the harvested power can be accurately modeled, yielding as a result guidelines in the design of the energy buffer. In order to provide these guidelines, the concept of energy utilization, measured in Energy-Erlangs, and the energy outage have been defined. The results show that the source-versatile, dynamics-decoupled model provides a more accurate model of the sensor node and shows how the energy buffer helps counteracting the impact of the temporal evolution of the harvested energy upon the energy outage probability, thus showing a strong compromise between performance and size. In addition to this, the spatial correlation of the energy has shown potential to develop novel transmission policies. As the results show, the spatial correlation of the energy field can help detecting unavailable neighboring nodes.

References

[1] A. Hajati, S. Bathurst, H. Lee, and S. Kim, "Design and fabrication of a nonlinear resonator for ultra wide-bandwidth energy harvesting applications," in *Proc. IEEE Int. Conf. Micro Electro Mechan. Syst.*, Jan. 2011, pp. 1301–1304.

[2] J. Hagerty, F. Helmbrecht, W. McCalpin, R. Zane, and Z. Popovic, "Recycling ambient microwave energy with broad-band rectenna arrays," *IEEE Trans. Microwave Theory Tech.*, vol. 52, no. 3, pp. 1014–1024, Mar. 2004.

[3] Y. K. Ramadass and A. P. Chandrakasan, "An efficient piezoelectric energy harvesting interface circuit using a bias-flip rectifier and shared inductor," *IEEE J. Solid-State Circuits*, vol. 45, no. 1, pp. 189–204, Jan. 2010.

[4] E. O. Torres and G. A. Rincón-Mora, "A 0.7-μm bicmos electrostatic energy-harvesting system IC," *IEEE J. Solid-State Circuits*, vol. 45, pp. 483–496, 2010.

[5] R. G. Cid-Fuentes, H. Martinez, A. Poveda, and E. Alarcon, "Electronically tunable switch-mode high-efficiency adaptive band-pass filters for energy harvesting applications," in *Proc. IEEE Int. Symp. Circuits Syst.*, May 2012, pp. 684–687.

[6] S. Bandyopadhyay and A. Chandrakasan, "Platform architecture for solar, thermal, and vibration energy combining with mppt and single inductor," *IEEE J. Solid-State Circuits*, vol. 47, no. 9, pp. 2199–2215, Sep. 2012.

[7] S. Sudevalayam and P. Kulkarni, "Energy harvesting sensor nodes: Survey and implications," *IEEE Commun. Surv. Tutorials*, vol. 13, no. 3, pp. 443–461, 2011.

[8] X. Jiang, J. Polastre, and D. Culler, "Perpetual environmentally powered sensor networks," in *Proc. 4th Int. Symp. Inf. Process. Sensor Netw.*, Apr. 2005, pp. 463–468.

[9] Y. Hu, Y. Zhang, C. Xu, L. Lin, R. L. Snyder, and Z. L. Wang, "Self-powered system with wireless data transmission," *Nano Lett.*, vol. 11, no. 6, pp. 2572–2577, 2011.

[10] R. Que, Q. Shao, Q. Li, M. Shao, S. Cai, S. Wang, and S.-T. Lee, "Flexible nanogenerators based on graphene oxide films for acoustic energy harvesting," *Angewandte Chemie*, vol. 124, no. 22, pp. 5514–5518, 2012.

[11] M. Gorlatova, A. Wallwater, and G. Zussman, "Networking low-power energy harvesting devices: Measurements and algorithms," in *Proc. IEEE INFOCOM*, Apr. 2011, pp. 1602–1610.

[12] R. Rajesh, V. Sharma, and P. Viswanath, "Information capacity of energy harvesting sensor nodes," in *Proc. IEEE Int. Symp. Inf. Theory*, Aug. 5, 2011, pp. 2363–2367.

[13] O. Ozel, K. Tutuncuoglu, J. Yang, S. Ulukus, and A. Yener, "Transmission with energy harvesting nodes in fading wireless channels: Optimal policies," *J. Sel. Areas Commun.*, vol. 29, pp. 1732–1743, Sep. 2011.

[14] D. Pech, M. Brunet, H. Durou, P. Huang, V. Mochalin, Y. Gogotsi, P.-L. Taberna, and P. Simon, "Ultrahigh-power micrometre-sized supercapacitors based on onion-like carbon," *Nature Nano*, vol. 5, no. 9, pp. 651–654, Sep. 2010.

[15] J. Jornet and I. Akyildiz, "Joint energy harvesting and communication analysis for perpetual wireless nanosensor networks in the terahertz band," *IEEE Trans. Nanotechnol.*, vol. 11, no. 3, pp. 570–580, May 2012.
[16] A. Kansal, J. Hsu, S. Zahedi, and M. B. Srivastava, "Power management in energy harvesting sensor networks," *ACM Trans. Embed. Comput. Syst.*, vol. 6, no. 4, pp. 32–38, Sep. 2007.
[17] A. Susu, A. Acquaviva, D. Atienza, and G. De Micheli, "Stochastic modeling and analysis for environmentally powered wireless sensor nodes," in *Proc. 6th Int. Symp. Model. Optimizat. Mobile, Ad Hoc, Wireless Netw. Workshops*, Apr. 2008, pp. 125–134.
[18] R. G. Cid-Fuentes, A. Cabellos, and E. Alarcon, "Energy harvesting enabled wireless sensor networks: Energy model and battery dimensioning," in *Proc. 7th Int. Conf. Body Area Netw.*, Oslo, Norway, Sep. 2012, pp. 131–134.
[19] C. Lu, V. Raghunathan, and K. Roy, "Efficient design of micro-scale energy harvesting systems," *IEEE J. Emerg. Sel. Topics Circuits Syst.*, vol. 1, no. 3, pp. 254–266, Sep. 2011.
[20] J. Ventura and K. R. Chowdhury, "Markov modeling of energy harvesting body sensor networks," in *Proc. IEEE 22nd Int. Symp. Personal Indoor Mobile Radio Commun.*, Toronto, Canada, Sep. 2011, pp. 2168–2172.
[21] S. Zhang and A. Seyedi, "Analysis and design of energy harvesting wireless sensor networks with linear topology," in *Proc. IEEE Int. Conf. Commun.*, Jun. 2011, pp. 1–5.
[22] B. Medepally, N. Mehta, and C. Murthy, "Implications of energy profile and storage on energy harvesting sensor link performance," in *IEEE Global Telecommun. Conf.*, Nov. 2009, pp. 1–6.
[23] M. Naderi, S. Basagni, and K. Chowdhury, "Modeling the residual energy and lifetime of energy harvesting sensor nodes," in *Proc. IEEE Global Commun. Conf.*, Dec. 2012, pp. 3394–3400.
[24] A. Seyedi and B. Sikdar, "Modeling and analysis of energy harvesting nodes in wireless sensor networks," in *Proc. 46th Annu. Allerton Conf. Commun., Control, Comput.*, Sep. 2008, pp. 67–71.
[25] R. G. Cid-Fuentes, M. Y. Naderi, R. Door, K. R. Chowdhury, and A. C.-A. Alarcón, "A duty-cycled random-phase multiple access scheme for wireless RF power transmission," *J. Publication*, 2014, submitted for publication.
[26] C. Park and P. Chou, "Ambimax: Autonomous energy harvesting platform for multi-supply wireless sensor nodes," in *Proc. 3rd Annu. IEEE Commun. Soc. Sensor Ad Hoc Commun. Netw.*, 2006, vol. 1, pp. 168–177.
[27] A. S. Weddell, M. Magno, G. V. Merrett, D. Brunelli, B. M. Al-Hashimi, and L. Benini, "A survey of multi-source energy harvesting systems," in *Proc. Design, Automat. Test Europe Conf. Exhibit.*, 2013, pp. 905–908.
[28] J. Medhi*, Stochastic Models in Queueing Theory*, A. Press, Ed. New York: Elsevier Science, 2003.
[29] T. S. Rappaport*, Wireless Communications Principles and Practices*. : Prentice-Hall, 2002.
[30] P. Nintanavongsa, U. Muncuk, D. Lewis, and K. Chowdhury, "Design optimization and implementation for RF energy harvesting circuits," *IEEE J. Emerg. Sel. Topics Circuits Syst.*, vol. 2, no. 1, pp. 24–33, Mar. 2012.
[31] M. Win, P. Pinto, and L. Shepp, "A mathematical theory of network interference and its applications," *Proc. IEEE*, vol. 97, no. 2, pp. 205–230, Feb. 2009.
[32] R. Mills and G. Prescott, "A comparison of various radiometer detection models," *IEEE Trans. Aerospace Electron. Syst.*, vol. 32, no. 1, pp. 467–473, Jan. 1996.
[33] R. G. Cid-Fuentes, A. Cabellos-Aparicio, and E. Alarcón, "Circuit area optimization for multiple energy harvester powered systems," in *Proc. IEEE Int. Symp. Circuits Syst.*, Melbourne, Australia, 2014.
[34] R. H. Jones and A. V. Vecchia, "Fitting continuous ARMA models to unequally spaced spatial data," *J. Am. Stat. Assoc.*, vol. 88, no. 423, pp. 947–954, 1993.
[35] J. O. Berger, V. D. Oliveira, and B. Sanso, "Objective bayesian analysis of spatially correlated data," *J. Am. Stat. Assoc.*, vol. 96, pp. 1361–1374, 2000.
[36] M. C. Vuran, O. B. Akan, and I. F. Akyildiz, "Spatio-temporal correlation: Theory and applications for wireless sensor networks," *Comput. Netw. J.*, vol. 45, pp. 245–259, 2004.
[37] R. Doost, K. Chowdhury, and M. Di Felice, "Routing and link layer protocol design for sensor networks with wireless energy transfer," in *Proc. IEEE GLOBECOM*, Dec. 2010, pp. 1–5.
[38] D. Hasenfratz, A. Meier, C. Moser, J.-J. Chen, and L. Thiele, "Analysis, comparison, and optimization of routing protocols for energy harvesting wireless sensor networks," in *IEEE Int. Conf. Sensor Netw., Ubiquitous, Trustworthy Comput.*, Jun. 2010, pp. 19–26.
[39] Z. A. Eu, H.-P. Tan, and W. K. G. Seah, "Opportunistic routing in wireless sensor networks powered by ambient energy harvesting," *Comput. Netw.*, vol. 54, no. 17, pp. 2943–2966, Dec. 2010.

Raul Gomez Cid-Fuentes (S'14) received the M.Sc. degree in telecommunications engineering, in 2011, from Universitat Politècnica de Catalunya (UPC), Barcelona, Spain, where he has been pursuing the Ph.D. degree at the Nanonetworking Center in Catalunya, since 2012.

In 2011 he was a visiting researcher at the Broadband Wireless Networking Lab, Georgia Institute of Technology, Atlanta, GA, USA. His current research interests are energy-harvesting-enabled wireless networks, wireless RF power transmission, and nanonetworks.

Albert Cabellos-Aparicio received the B.Sc., M.Sc., and Ph.D. degrees in computer science engineering from the Universitat Politècnica de Catalunya (UPC), Barcelona, Spain, in 2001, 2005, and 2008, respectively.

In September 2005, he became an Assistant Professor of the Computer Architecture Department and as a Researcher in the Broadband Communications Group. In 2010, he joined the Nanonetworking Center in Catalunya, where he is the Scientific Director. He is an Editor of the Elsevier journal on *Nano Computer Networks*, *Computer Networks* and member of the Project Management Committee of the LISPmob opensource initiative. He has been a visiting professor at Royal Institute of Technology (KTH) (2012) and the Massachusetts Institute of Technology (2013). His main research interests are future architectures for the internet and nanonetworks.

Eduard Alarcón (M'04) received the M.Sc. (national award) and the Ph.D. degrees (honors) in electrical engineering from the Technical University of Catalunya (UPC BarcelonaTech), Barcelona, Spain, in 1995 and 2000, respectively.

Since 1995, he has been with the Department of Electronic Engineering at UPC, where he became Associate Professor in 2000. From August 2003 to January 2004, July to August 2006, and July to August 2010 he was a Visiting Professor at the CoPEC Center, University of Colorado, Boulder, CO, USA, and during January to June 2011 he was Visiting Professor at the School of ICT/Integrated Devices and Circuits, Royal Institute of Technology (KTH), Stockholm, Sweden. During the period 2006–2009 he was Associate Dean of International Affairs at the School of Telecommunications Engineering, UPC. He has co-authored more than 300 scientific publications, five books, six book chapters, and five patents, and has been involved in different national, European, and USA (DARPA, NSF) R&D projects within his research interests including the areas of on-chip energy management circuits, energy harvesting, and wireless energy transfer, and nanotechnology-enabled wireless communications. He was the invited co-editor of a special issue of the *Analog Integrated Circuits and Signal Processing* journal devoted to current-mode circuit techniques and a special issue of the *International Journal on Circuit Theory and Applications*. He currently serves as Associate Editor for Elsevier's *Nano Communication Networks* journal (2009 to present) and the *Journal of Low Power Electronics* (2011 to present).

Dr. Alarcón has given 30 invited or plenary lectures and tutorials in Europe, America, and Asia, was appointed by the IEEE CAS society as distinguished lecturer for 2009–2010 and lectures yearly MEAD courses at EPFL. He has participated in Evaluation Boards for research proposals both in Europe (Chist-ERA, Belgium, Ireland, Italy) America (Canada), and Asia (Korea). He is elected member of the IEEE CAS Board of Governors (2010–2013, 2014 to

present) and member of the IEEE CAS long term strategy committee. He was recipient of the Myril B. Reed Best Paper Award at the 1998 IEEE Midwest Symposium on Circuits and Systems. He was the invited Associate Editor for a IEEE TPELS special issue on PwrSOC. He co-organized special sessions related to on-chip power management at IEEE ISCAS03, IEEE ISCAS06, and NOLTA 2012, and lectured tutorials at IEEE ISCAS09, ESSCIRC 2011, IEEE VLSI-DAT 2012, and APCCAS 2012. He was the 2007 Chair of the IEEE Circuits and Systems Society Technical Committee on Power Circuits. He was the technical program co-Chair of the 2007 European Conference on Circuit Theory and Design–ECCTD07 and of LASCAS 2013, Special Sessions co-Chair at IEEE ISCAS 2013, tutorial co-Chair at ICM 2010, Demo Chair of BodyNets 2012, track co-Chair of IEEE ISCAS 2007, IEEE MWSCAS07, IEEE ISCAS 2008, ECCTD'09, IEEE MWSCAS09, IEEE ICECS'2009, ESSCIRC 2010, PwrSOC 2010, IEEE MWSCAS12, and TPC member for IEEE WISES 2009, WISES 2010, IEEE COMPEL 2010, IEEE ICECS 2010, IEEE PRIME 2011, ASQED 2011, ICECS 2011, INFOCOM 2011, MoNaCom 2012, LASCAS 2012, PwrSOC 2012, ASQED 2012, IEEE PRIME 2012, IEEE iThings 2012, and CDIO 2013. He served as an Associate Editor of the IEEE TRANSACTIONS ON CIRCUITS AND SYSTEMS—PART II: EXPRESS BRIEFS (2006–2007), Associate Editor of the IEEE TRANSACTIONS ON CIRCUITS AND SYSTEMS—PART I: REGULAR PAPERS (2006–2012) and in the founding Senior Editorial Board of the IEEE *Journal on Emerging and Selected Topics in Circuits and Systems* (2010–2013).